Permethyltitanocene Derivatives with Naked Chalcogen Ligands: Synthesis of $[(Cp_2^*Ti)_2(\mu\text{-}E)]$ and $[Cp_2^*Ti(\eta^2\text{-}E_2)]$ and the Role of the Terminal Chalcogenides $[Cp_2^*Ti(E)]$ in Their Interconversion (E = Se, Te)

Jason M. Fischer, Warren E. Piers,* Tom Ziegler,* Leonard R. MacGillivray and Michael J. Zaworotko

Abstract: Permethyltitanocene hydride, $[Cp_2^*TiH]$, reacts with elemental selenium or tellurium to give the products $[(Cp_2^*Ti)_2(\mu\text{-}E)]$ (E = Se, **1a**; Te, **1b**), $[Cp_2^*Ti(\eta^2\text{-}E_2)]$ (E = Se, **2a**; Te, **2b**) and $[Cp_2^*Ti(\eta^2\text{-}Se_3)]$ (**3**), depending on the equivalency of the chalcogen employed. Dinuclear compounds **1** are paramagnetic and have D_{2d} (idealized) structures, as shown by X-ray structural analysis of μ-telluride **1b**; they may be converted to diamagnetic dichalcogenides **2** through further reaction with the appropriate chalcogen. Derivatives **2** are monomeric in the solid state, as shown by X-ray structural analysis of ditelluride **2b**, and in solution, as demonstrated by multinuclear NMR spectroscopy. Combination of diselenide **2a** and ditelluride **2b** results in partial redistribution to the mixed species $[Cp_2^*Ti(\eta^2\text{-}SeTe)]$, suggesting dimeric structures of formula $[Cp_2^*Ti(\mu\text{-}E\text{-}E)_2TiCp_2^*]$ may be accessible in solution. The dichalcogenides and the triselenide may be converted back to complexes **1** by treatment with a chalcogen-abstracting agent. The possible involvement of monomeric terminal chalcogenides $[Cp_2^*Ti(E)]$ in the interconversion of **1** and **2** was probed experimentally and computationally by means of Density Functional Theory calculations on $[Cp_2M(E)]$ (M = Ti, E = O, S, Se, Te; M = Zr, E = O, Te). Several unsuccessful attempts to generate and trap $[Cp_2^*Ti(Te)]$ are described. The results of these studies suggest that $[Cp_2^*Ti(Te)]$ has a very weak Ti–Te bond and a readily accessible triplet excited state. These factors, along with the small size of titanium, render this member of the $[Cp_2^*M(E)]$ family of complexes difficult to trap with Lewis bases, in contrast to many other congeners in the series of Group 4 terminal chalcogenides.

Keywords
chalcogen compounds · metallocenes · selenium compounds · tellurium compounds · titanium complexes

Introduction

Group 4 bent metallocene complexes of polychalcogenide ligands occupy a prominent position in the development of the coordination chemistry of E_n^{2-} ligands (E = S, Se; $n = 3$, ≥ 5).[1] For example, bis(cyclopentadienyl)titanium pentasulfide, $[Cp_2TiS_5]$, is, next to ferrocene, one of the best-known organometallic compounds, and its ease of preparation[2] and fluxional properties[3] have made it the focus of much study even at the undergraduate level. Since the size of the polysulfide or polyselenide ring can be varied through modification of the steric properties of the cyclopentadienyl donors and/or the nature of the polychalcogenide reagent, these compounds are valued as starting materials for synthesis of chalcogen-rich heterocycles.[4]

More recently, zirconocene and hafnocene derivatives of less catenated chalcogenide ligands E_n^{2-} ($n = 1$, 2 or 3) have been generated and trapped as Lewis base stabilized adducts ($n = 1$, 2[5]) or prepared as base-free species ($n = 3$[6]). Structural characterization of each member of the series of compounds $[(C_5Me_4R)_2M(E)(py)]$ (R = Me or Et; M = Zr, Hf; py = NC_5H_5) has deepened our understanding of the properties of metal–ligand multiple bonds.[5] The completeness of experimental data for this family of compounds has attracted interest from Cundari's computational group, which found that geometrical parameters can be calculated with a high degree of accuracy for transition-metal complexes of this type by means of Effective Core Potential (ECP) methods.[7] In contrast, only one member of the titanium series of terminal chalcogenides has been reported, the oxo derivative $[Cp_2^*Ti(O)(4\text{-phenyl-py})]$.[8]

Around the time these reports began to appear, we became interested in developing the chemistry of titanocene complexes with telluride and polytelluride ligands, which, in spite of the rich chemistry associated with polysulfide derivatives of titanocene, was relatively unexplored. We gained entry into this chemistry[9] by reaction of Teuben's permethyltitanocene hydride $[Cp_2^*TiH]$ ($Cp^* = C_5Me_5$) with elemental tellurium.[10] Our interest in the products of this reaction stems from their potential utility as both stoichiometric[9] and catalytic[11] tellurium transfer agents for inorganic synthesis.

[*] Prof. W. E. Piers, Prof. T. Ziegler
Department of Chemistry, The University of Calgary
2500 University Drive N. W., Calgary, Alberta, T2N 1N4 (Canada)
Fax: Int. code + (403) 289-9488
email: wpiers@chem.ucalgary.ca; ziegler@chem.ucalgary.ca
J. M. Fischer
Department of Chemistry and Biochemistry, University of Guelph
Guelph, Ontario N1G 2W1 (Canada)
Prof. M. J. Zaworotko, L. R. MacGillivray
Department of Chemistry, Saint Mary's University
Halifax, Nova Scotia B3H 3C3 (Canada)

  0947-6539/96/0210-1221 $ 15.00+.25/0

In the light of Parkin's work[5a] and Andersen's terminal-oxo permethyltitanocene derivative,[8] it seemed reasonable to expect the involvement of terminal chalcogenides, [Cp^*_2Ti(Se,Te)], in the reactions of [Cp^*_2TiH] with tellurium and selenium reported herein. However, several experiments designed to trap the permethytitanocene terminal tellurido complex were unsuccessful. These observations led us to probe the [Cp_2Ti–E] series of compounds computationally by means of Density Functional Theory (DFT). In addition to providing accurate geometrical information, these methods allow for some assessment of thermodynamic parameters, such as bond energies and the energy separation between different electronic states. The results of these computations provide insight into why [Cp^*_2Ti(Te)] is so difficult to trap by methods known to be effective for capturing the zirconium and hafnium congeners.[5]

Results and Discussion

Reactions of [Cp^*_2TiH] with selenium and tellurium: Permethyltitanocene hydride reacts with selenium or tellurium powder to form naked chalcogenide or polychalcogenide complexes, depending on the equivalency of chalcogen (E) used in the reaction (Scheme 1). Tellurium-containing products were in some cases more conveniently prepared from tributylphosphine telluride as a source of soluble tellurium.

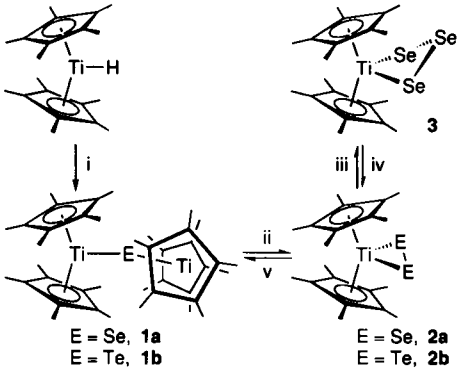

Scheme 1. i) Se or Te; ii) Se (E = Se) or Te=PBu_3 (E = Te); iii) Se, E = Se; iv) PPh_3; v) PMe_3 (E = Se) or Hg(o) (E = Te).

When [Cp^*_2TiH] was treated with 0.5 equivalents of Se or Te, the products were the dimeric μ-chalcogenides [(Cp^*_2Ti)$_2$(μ-E)] (E = Se, **1a**; E = Te, **1b**) and dihydrogen. Because of the paramagnetism of these d^1–d^1 compounds, the NMR spectra comprised one broad resonance (**1a**, δ = 15.4; **1b**, δ = 15.9) for the Cp* rings that, though featureless, was nonetheless diagnostic. We have not probed the magnetic properties of **1a** and **1b** in any detail but the data we have accumulated suggest a picture for the bonding and electronic structure of chalcogenides **1** similar to that developed by Lukens and Andersen in a more comprehensive fashion for the closely related compound [(Cp_2Ti)$_2$(μ-O)].[12] A qualitative picture of the bonding in this compound (and by extension **1a** and **1b**) predicts that the unpaired electrons reside in the nonbonding (with respect to oxygen) $1a_1$ metallocene orbitals on each titanium. Thus, superexchange pathways through the bridging oxo ligand are not possible. Additionally, the orthogonal nature of the $1a_1$ SOMOs on each metal preclude through-space antiferromagnetic coupling, owing to the (idealized) D_{2d} structure of the compound.[13] Other experiments showed that the depressed value of μ_{eff} for [(Cp_2Ti)$_2$(μ-O)] (2.47 μ_B) was caused by intermolecular ferromagnetic coupling. Variable-temperature susceptibility measurements on **1b** showed that, between the range of 80–250 K, normal Curie–Weiss behaviour was followed (θ = –25.6 K, μ_{eff} = 2.1 μ_B per molecule). A maximum at about 4 K was observed in the $1/\chi$ vs. T plot; however, caution in drawing conclusions based on this plot must be advised owing to the low number of data points defining this maximum. Clearly antiferromagnetic coupling, if present, is very weak in **1b**. The low observed magnetic moment for **1b** may therefore be a result of intermolecular interactions, a notion which is supported by the non-zero value of θ[14, 15] and the results obtained for the μ-oxo species [(Cp_2Ti)$_2$(μ-O)].[12]

Structurally, compounds **1a** and **1b** have the same "allene-like" D_{2d} symmetry found in other related molecules with chalcogenides bridging two bent metallocene fragments.[13, 16] Figure 1 shows an ORTEP diagram of μ-telluride **1b** along with

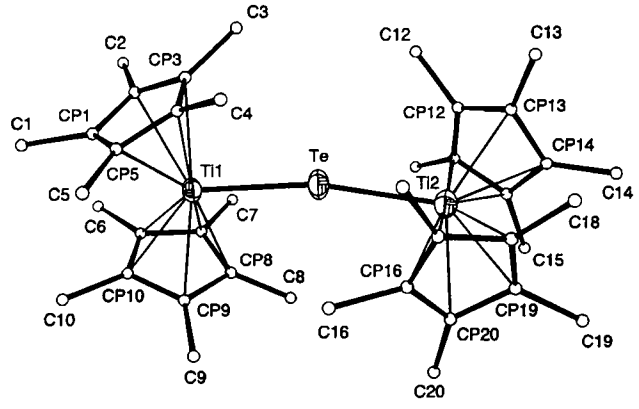

Fig. 1. ORTEP diagram of [(Cp^*_2Ti)$_2$(μ-Te)], **1b**. Selected bond lengths (Å): Ti1–Te, 2.705(3); Ti2–Te, 2.697(3); Ti1–Cp_{cent}, 2.0909(23), 2.1085(23); Ti2–Cp_{cent}, 2.124(3), 2.085(5). Selected bond angles (°): Ti1-Te-Ti2, 168.62(8); Cp_{cent}-Ti1-Cp_{cent}, 140.29(11); Cp_{cent}-Ti2-Cp_{cent}, 140.82(12). Dihedral angle between planes containing Cp_{cent}-Ti-Cp_{cent}: 94.6°.

selected metrical data. The orthogonal $Cp_{centroid}$–Ti–$Cp_{centroid}$ planes allow for optimal π overlap between the empty orbitals of b_2 symmetry[17] on the metallocene fragments and the occupied unhybridized p orbitals of the tellurium atom. Consequently, the Ti–Te distances observed (2.705(3) and 2.697(3) Å) are ca. 0.1–0.2 Å shorter than known Ti–Te bonds with orders of one[11, 18] and lengths of 2.8–2.9 Å. Although no structurally characterized examples of Ti=Te have been reported, calculated values of 2.592 (vide infra) and 2.58 Å[19] are available. Thus, the Ti–Te bonds in **1b** have an order of ca. 1.5 based on the observed Ti–Te separations of about 2.7 Å.

X-ray quality crystals of **1a** were also obtained, but the data set collected could not be refined to a satisfactory R value owing to severe disorder in the Cp* rings. Nonetheless, the gross features of the molecule were apparent and clearly showed that the Cp^*_2Ti fragments were set at about 90° to each other, suggesting a bonding picture for the μ-selenide complex similar to that developed for [(Cp_2Ti)$_2$(μ-O)].[12]

Referring again to Scheme 1, these paramagnetic complexes react further with chalcogen to form the diamagnetic dichalcogenides [Cp^*_2Ti(η^2-E_2)] (E = Se, **2a**; Te, **2b**). These materials were volatile and thermally stable enough to be purified by means of vacuum sublimation and characterized by mass-spectroscopic methods. Parent peaks at m/e = 478 and 574 for **2a**

0947-6539/96/0210-1222 $ 15.00+.25/0 Chem. Eur. J. 1996, 2, No. 10

and **b**, respectively, indicated that these compounds were monomeric in the vapour phase; X-ray structural analysis of **2b** (Fig. 2) revealed a monomeric solid state structure. The nuclearity of these compounds is at issue since dimers of "$[Cp'_2Ti(\eta^2\text{-}E_2)]$" ($[Cp' = C_5H_4Me]$ incorporating the less bulky methylcyclopentadienyl donor have been reported.[20] These compounds

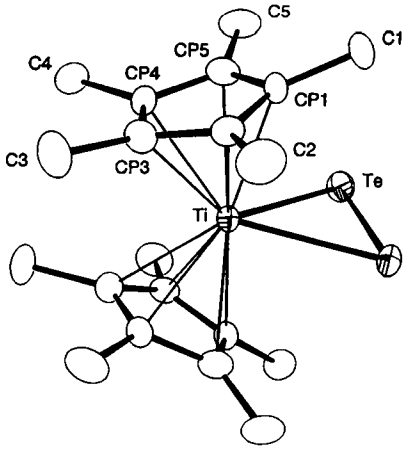

Fig. 2. ORTEP diagram of $[Cp^*_2Ti(\eta^2\text{-}Te_2)]$, **2b**. Selected bond lengths (Å): Ti–Te, 2.808(3); Te–Te(a), 2.7030(18); Ti–Cp_{cent}, 2.1046(12). Selected bond angles (°): Te(a)-Te-Ti, 61.23(4); Te-Ti-Te(a), 57.53(7); Cp_{cent}-Ti-Cp_{cent}, 140.45(16).

are of general formula $[Cp'_2Ti(\mu\text{-}E\text{-}E)_2TiCp'_2]$ with a six-membered 1,4-Ti_2E_4 ring that adopts a rigid chair conformation at room temperature. Although the possibility of $[Cp'_2Ti(\eta^2\text{-}Se_2)]$ intermediates was raised,[4a] no evidence was obtained to support their presence in these systems. Evidently the bulkier Cp* ligand favours the monomer over the dimeric structure in diselenide **2a** and ditelluride **2b**.

The bonding in compounds **2** may be viewed in a classical Dewar–Chatt–Duncanson manner, in which singlet E=E (isolobal with ethylene) donates σ electron density to $[Cp^*_2Ti]$, which π back-donates into empty π* orbitals on E_2. In accord with this picture, the Te–Te distance of 2.7030(18) Å in **2b** lies midway between the Te–Te distances in Te_2 (2.59(2) Å[21]) and elemental tellurium (2.835 Å[22]) for a bond order of approximately 1.5. Unlike the zirconium analogs of **2**, which retain a CO ligand in their preparation from $[Cp^*_2Zr(CO)_2]$ and E,[6] neither **2a** nor **2b** binds CO strongly. When **2b** was treated with an excess of CO (1 atm), the dicarbonyl complex $[Cp^*_2Ti(CO)_2]$ and Te(0) were the only products observed.

Solution ^{77}Se and ^{125}Te NMR data (Table 1) do not necessarily support a monomeric structure in solution, given the wide range of chemical shifts observed for η^2-Se_2[23] and η^2-Te_2[24] ligands in other complexes. However, the closeness of the observed chemical shifts for the ^{125}Te nucleus of **2b** in solution (C_6D_6, $\delta = 1463$) and in the solid state (powder sample, $\delta = 1480$) supports a monomeric solution structure. Based on empirically observed relationships between ^{125}Te chemical shifts and those of ^{77}Se nuclei in structurally analogous complexes,[25] the observed ^{77}Se chemical shift for **2a** is consistent with a monomeric structure as well.

Table 1. $^{77}Se\{^1H\}$ and $^{125}Te\{^1H\}$ NMR data.

Compound		δ Se [a]	δ Te [b]	$^1J_{E\ E}$ [c]
$[Cp^*_2Ti(\eta^2\text{-}Se_2)]$	**2a**	1252		
$[Cp^*_2Ti(\eta^2\text{-}Te_2)]$	**2b**		1463 1480 [d]	1603
$[Cp^*_2Ti(\eta^2\text{-}SeTe)]$	**2c**	992	2012	683
$[Cp^*_2Ti(\eta^2\text{-}Se_3)]$	**3**	813, 322 [e]	–	162

[a] C_6D_6, relative to Me_2Se at $\delta = 0.0$. [b] C_6D_6, relative to Me_2Te at $\delta = 0.0$. [c] Hz. [d] Powder sample referenced to Me_2Te at $\delta = 0.0$. [e] Present in a 2:1 ratio.

The diselenide and ditelluride compounds may be converted back to their respective μ-chalcogenides by treatment with PMe_3 for E = Se or elemental mercury for E = Te. The diselenide reacts further with elemental selenium to generate the triselenide **3** (Scheme 1); no analogous reaction occurs between either **2a** or **2b** and tellurium; this is probably a reflection of the lack of available space in the permethyltitanocene girdle for accommodating polychalcogenide ligands. The triselenide **3** was characterized by its ^{77}Se NMR spectrum, in which signals at $\delta = 813$ and 322, found in a 2:1 ratio, were observed ($^1J(Se,Se) = 162$ Hz). The four-membered $TiSe_3$ ring is likely to be puckered as in the related complexes $[Cp^*_2Ti(\eta^2\text{-}S_3)]$[26] and $[Cp^*_2Zr(\eta^2\text{-}E_3)]$ (E = S, Se, Te),[6] although at room temperature the Cp* environments are averaged. Treatment of **3** with a less basic phosphine such as Ph_3P allowed for clean conversion to $[Cp^*_2Ti(\eta^2\text{-}Se_2)]$, uncontaminated by paramagnetic $[(Cp^*_2Ti)_2(\mu\text{-}Se)]$.[27]

When equimolar amounts of the **2a** and **2b** were mixed together in C_6D_6 and heated at 40 °C, partial redistribution to the mixed chalcogenide complex $[Cp^*_2Ti(\eta^2\text{-}SeTe)]$, **2c**, was observed [Eq. (1)]. Alternatively, this compound could be generated as the major constituent (60%) of a mixture by treatment of the diselenide **2a** with one equivalent of $Te{=}PBu_3$ [Eq. (2)] and

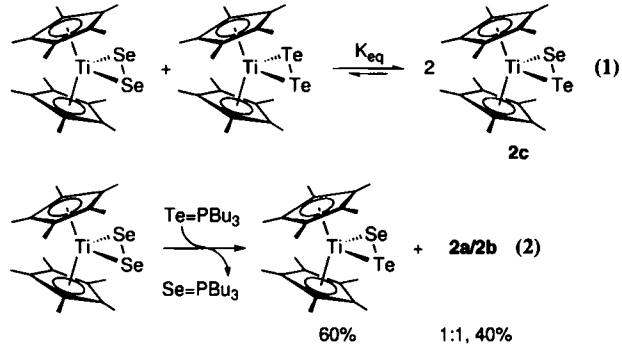

characterized by solution NMR techniques. In accord with expectations based on the relative electronegativities of Se and Te, the resonance for the ^{77}Se nucleus in **2c** shifts upfield relative to that in **2a**, while the ^{125}Te shift moves to lower field as compared with that in **2b**.

The mechanism of the redistribution reaction of Equation (1) is not known but intermediates related to the $[Cp'_2Ti(\mu\text{-}E\text{-}E)_2TiCp'_2]$ compounds mentioned above are probably involved. While Rauchfuss et al. found no crossover when the compounds $[Cp'_2Ti(\mu\text{-}Se\text{-}Se)_2TiCp'_2]$ and $[(C_5H_4iPr)_2Ti(\mu\text{-}Se\text{-}Se)_2Ti(C_5H_4iPr)_2]$[4a] were mixed, the observations of Equation (1) above clearly show that dimeric intermediates are accessible to **2a** and **2b** in solution. Two approaches to these dimers from monomers **2a/b** may be proffered (Scheme 2). In one model, Scheme 2A, the chairlike dimer is formed directly when one monomer approaches the other from the top (or bottom) of the E–E bond. This is an orbitally allowed process, and isomerization of the resulting chair leads to **2c**. In the other model, Scheme 2B, a bimolecular step involving a lateral approach and coordination of chalcogen lone pairs to the empty in-plane $1a_1$ LUMO[17] on the metal results in a σ-bond metathesis-type

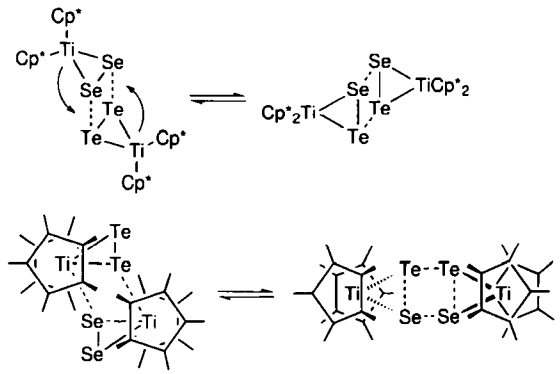

Scheme 2. Two possible mechanisms for the redistribution reaction in Equation (1).

reaction leading to the dimeric precursor to **2c**. Again, the bulk of the Cp* rings forces this dimer to dissociate into the observed mixed monomer **2c**. At 40 °C, equilibrium is reached such that $K_{eq} \approx 9$ for Equation (1).

Attempted generation and capture of [Cp$_2^*$Ti(Te)]: The conversion of the paramagnetic complexes **1** to the diamagnetic dichalcogenides **2** is a mechanistically intriguing reaction. Most chemically plausible paths invoke at some point the (probably) diamagnetic terminal chalcogenide species "[Cp$_2^*$Ti(E)]". In the light of the series of Lewis base stabilized zirconium and hafnium terminal chalcogenides characterized by Parkin[5a,b] and Bergman[5c,d] and Andersen's terminal-oxo complex [Cp$_2^*$Ti(O)(4-phenyl-py)],[8] [Cp$_2^*$Ti(Se,Te)] intermediates seem entirely likely to be involved in this chemistry. Furthermore, the observation of a molecular ion peak corresponding to [Cp$_2^*$Ti(Se)]$^\bullet$ (m/e = 397) in the mass spectrum of **2a** hinted at the accessibility of the selenide; no indication for [Cp$_2^*$Ti(Te)] was in evidence in the mass spectrum of ditelluride **2b**, however.

The experiments outlined in Equations (3–8) show our attempts to trap [Cp$_2^*$Ti(Te)]. The presence of pyridine had no effect on the result of the reaction between **1b** and Te=PBu$_3$ [Eq. (3)]. Direct reaction between permethyltitanocene[28] and the tellurium transfer reagent [Eq. (4)] led only to mixtures of **1b** and **2b**, depending on the equivalency of tellurium employed; lowering of reaction temperature did not alter the outcome, and pyridine was not compatible with [Cp$_2^*$Ti]. Use of Parkin's strategy of masking the permethylmetallocene as the dicarbonyl adduct[5a] was not effective for titanium chemistry [reaction (5)]. Perhaps most significantly, heating the products of reaction (5) in the presence of excess pyridine resulted in generation of μ-telluride compound **1b** with loss of elemental tellurium [Eq. (6)]. This is the only reaction in the series that might be expected to generate [Cp$_2^*$Ti(Te)] in the absence of either excess Te or "[Cp$_2^*$Ti]" (in an unmasked form). The last two experiments were also designed to intercept the terminal telluride after tellurium atom abstraction from the η^2-ditelluride and also failed to yield [Cp$_2^*$Ti(Te)(py)].[29]

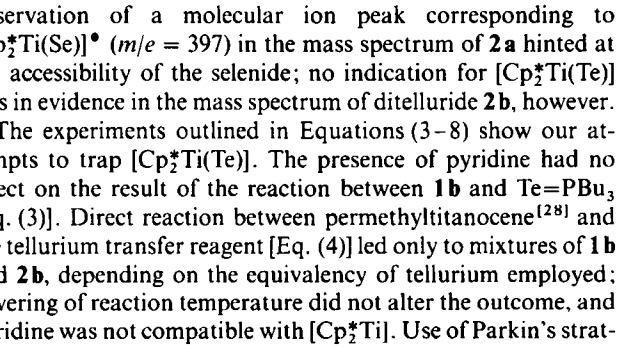

These results suggest that [Cp$_2^*$Ti(Te)] is either thermodynamically inaccessible or kinetically highly reactive. Indeed, it is possible that both thermodynamic and kinetic factors are involved, in the light of the reducing nature of the Te^{2-} ligand and the relatively accessible lower oxidation states of titanium in comparison to zirconium and hafnium. In combination, these two attributes of the Ti,Te member of the [Cp$_2^*$M(E)] series of compounds might be expected to increase the importance of resonance structures such as **A** or **B** relative to **C** (Scheme 3) in

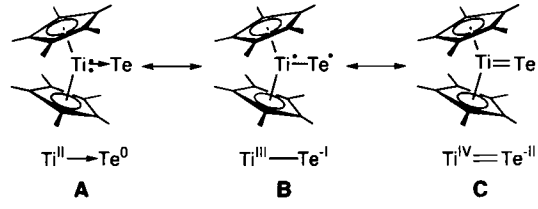

Scheme 3. Resonance structures for [Cp$_2^*$Ti(Te)].

its structure, leading to a fundamentally weaker Ti–Te bond and/or a high degree of kinetic instability in the presence of reagents with a triplet ground state (i.e., permethyltitanocene or elemental tellurium[30]). We decided to probe these questions with DFT calculations on the molecular and electronic structures of [Cp$_2$Ti–E] (E = O, S, Se, Te). For comparison with the titanium series and with experimental and ECP computational results[7] on the zirconium congeners, calculations were also performed on [Cp$_2$Zr–E] for E = O and Te.

Computational results: The frontier orbitals of the Cp$_2$M fragment have been studied by various methods (Fig. 3).[17] We find the d^2 fragments Cp$_2$M (M = Ti, Zr) to have $^3B_2$ triplet ground states with $(1a_1)^1(1b_2)^1$ configurations. Slightly higher in energy (at 2.9 and 21.9 kJ mol^{-1} for Ti and Zr, respectively) is a $^3A_1$ state ($(1a_1)^1(2a_1)^1$). The lowest-energy singlet state is $^1A_1$ ($1a_1^2$) and is, respectively, 58.6 (Ti) and 46.2 (Zr) kJ mol^{-1} above the $^3B_2$ ground state (Table 2). Also shown are the optimized geometries for the different states of Cp$_2$M.

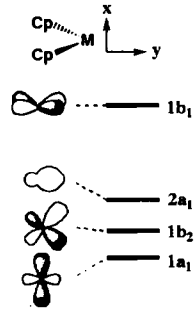

Fig. 3. Frontier orbitals of the bent metallocene fragment Cp$_2$M.

Table 2. Optimized structures and relative energies for different states of [Cp$_2$M] (M = Ti, Zr).

State		R(M–Cp) [a] Ti	Zr	Cp-M-Cp [a] Ti	Zr	Rel. energies [b] Ti	Zr
$^1A_1$	$(1a_1)^2$	1.985	2.153	163	149.4	58.6	46.2
$^3A_1$	$(1a_1)^1(2a_1)^1$	2.053	2.188	169.1	142.4	2.9	21.9
$^3B_2$	$(1a_1)^1(1b_2)^1$	2.025	2.154	169.2	151.4	0.0	0.0

[a] Lengths in Å and angles in degrees. [b] kJ mol^{-1}.

© VCH Verlagsgesellschaft mbH, D-69451 Weinheim, 1996 0947-6539/96/0210-1224 $ 15.00+.25/0 Chem. Eur. J. 1996, 2, No. 10

Using the d^2 metallocene fragments thus optimized, we studied the interaction between Cp_2M and E. With idealized C_{2v} structures in which the M–E bond points along the C_2 axis, all the Cp_2ME systems under investigation were found to have a singlet ground state. Formation of the Cp_2M–E bond may be formally viewed as being formed from the Cp_2M fragment promoted to its $^1A_1$ $(1a_1)^2$ singlet state and E promoted from its ^3P ground state to its $s^2(p_\pi)^2(p_\sigma)^0$ valence state with p_σ pointing along the M–E bond vector. The M–E bond is formed by donation of charge from $1a_1$ of Cp_2M to p_σ of E along with two π back-donation components from the orthogonal p_π orbitals on E to the $1b_2$ and $1b_1$ acceptor MOs on Cp_2M (Fig. 4).

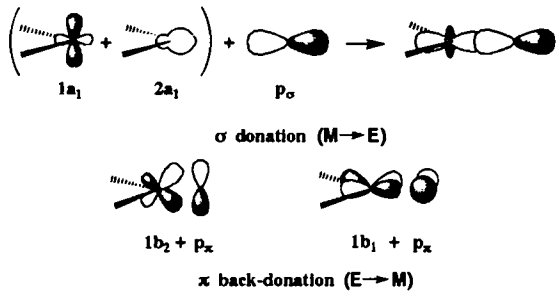

Fig. 4. Bonding interactions in Cp_2M–E (M = Ti, Zr; E = O, S, Se, Te).

In order to analyze the interaction between the chalcogenides and the metal fragments Cp_2M in a more detailed way, we employed the extended transition state (ETS) method.[31] The ETS scheme allows the Cp_2M–E bond energy $D(Cp_2Ti–E)$ to be expressed as the sum of three energy terms [Eq. (9)]. In this

$$D(Cp_2M–E) = E_{steric} + E_{prep} + E_{orb} \quad (9)$$

description, E_{steric} represents the steric interaction energy between fragments Cp_2M and E and stems from the electrostatic interaction E^0 between the two fragments as well as the repulsive Pauli contribution, E_{Pauli}, because of the two-orbital–four-electron repulsive Pauli interactions between occupied orbitals on the two fragments.[32] The term E_{prep} comes from the energy required to promote E and Cp_2M to their respective valence states. An extra contribution results from relaxing the structure of Cp_2M to the geometry adopted in the Cp_2M–E complex.

The E_{orb} term in Equation (9) originates from the bonding interaction between occupied and virtual orbitals on the two fragments. This term can be divided further into contributions from different symmetry representations (Γ_i) of the C_{2v} molecular point group preserved during the formation of Cp_2M–E from E and Cp_2M [Eq. (10)].[33] Here E_{a1} is the contribution to the Cp_2M–E bond energy from σ-donation, M → E, whereas E_{b1} and E_{b2} are the corresponding contributions from the π back-donation (Fig. 4).

$$E_{orb} = E_{a1} + E_{b1} + E_{b2} \quad (10)$$

Table 4. Optimized geometrical parameters [a] for $[Cp_2M–E]$ and calculated triplet/singlet separations.

$[Cp_2M–E]$	M–Cp [a]	Cp-M-Cp [a]	R(Ti–E)	$E_{trip} - E_{sing}$ [c]
$[Cp_2TiO]$	2.153 (2.093) [b]	135.9 (140.4)	1.665 (1.734)	134.7
$[Cp_2TiS]$	2.116	136.9	2.154	
$[Cp_2TiSe]$	2.095	137.6	2.305	
$[Cp_2TiTe]$	2.082 (2.053)	138.9 (140.6)	2.592 (2.659)	18.4
$[Cp_2ZrO]$	2.277 (2.251)	135.2 (140.8)	1.799 (1.896)	164.9
$[Cp_2ZrTe]$	2.239 (2.197)	137.3 (140.3)	2.696 (2.823)	32.3

[a] Lengths in Å and angles in degrees. [b] Numbers in parentheses are for the optimized triplet states. [c] kJ mol^{-1}.

The factors making up the Cp_2M–E bond energies are given in Table 3; Table 4 gives key parameters for the optimized structures of $[Cp_2M–E]$. The calculated metrical data for the singlet ground states of $[Cp_2M–E]$ are in close agreement with experimentally determined values for pyridine adducts of $[Cp^*_2M–E]$, where available.[5a, 8] For the M = Ti series, the destabilizing E^0 term (E_{steric}) decreases from O to Te within the Group 16 elements as the Cp_2M–E distance becomes larger. The trend in the dominant stabilizing factor in M–E bond formation, the M → E σ donation represented by the term E_{a1}, shows that the E_{a1} transfer is also largest for E = O and decreases in absolute terms towards Te, which has the *n*p orbitals of highest energy. The driving force for this interaction is the transfer of charge from the high-energy $1a_1$ metallocene orbital to the lower energy *n*p chalcogen orbitals. Stabilization derived from the in-plane π back-donation is an order of magnitude lower than the E_{a1} component but remains roughly constant over the chalcogen series because the rise in the energies of the donor *n*p orbitals compensate for the increasing M–E distances over the series. Since the out-of-plane b_1 metal acceptor orbital is higher in energy, the E_{b1} energetic component of the bond is less important than E_{b2}. Both of these π back-donating interactions serve to dissipate the negative charge buildup on the chalcogen that arises from the σ donation E_{a1}.

A population analysis for the three primary M–E interactions (Table 5) shows that this charge buildup is greatest for oxygen, in agreement with Parkin's suggestion of a significant ionic component to the Zr–O bond of $[Cp^{Et}_2Zr(O)py]$ in comparison to the heavier congeners of the series.[5a] The amount of

Table 5. Population analysis.

$[Cp_2M–E]$	σ donation M → E	π back-donation E → M_{b2}	E → M_{b1}	$\sigma - \pi$
$[Cp_2TiO]$	1.66	0.51	0.39	0.76
$[Cp_2TiS]$	1.52	0.66	0.30	0.56
$[Cp_2TiSe]$	1.41	0.70	0.26	0.45
$[Cp_2TiTe]$	1.37	0.76	0.19	0.42
$[Cp_2ZrO]$	1.53	0.49	0.35	0.69
$[Cp_2ZrTe]$	1.48	0.66	0.26	0.56

Table 3. Breakdown of the calculated $[Cp_2M–E]$ bond energies [a].

$Cp_2M–E$	E^M_{prep}	E^E_{prep}	E_{el}	E_{Pauli}	E^0	E_{a1}	E_{b2}	E_{b1}	$D(Cp_2M–E)$ [b]
$[Cp_2TiO]$	152.6	272.1	−309.1	1251.7	942.6	−1802.0	−94.1	−70.5	−599.2
$[Cp_2TiS]$	140.1	155.7	−369.7	944.6	574.9	−1121.0	−93.2	−47.1	−390.9
$[Cp_2TiSe]$	133.9	140.7	−429.5	909.2	479.8	−972.9	−84.10	−34.4	−337.0
$[Cp_2TiTe]$	130.3	122.4	−514.6	935.7	421.1	−806.8	−93.8	−31.7	−258.5
$[Cp_2ZrO]$	75.6	272.1	−173.1	745.0	571.9	−1452.1	−45.7	−49.4	−627.6
$[Cp_2ZrTe]$	62.5	122.4	−169.1	395.0	225.9	−693.0	−57.0	−29.2	−368.2

[a] Energies in kJ mol^{-1}. [b] $D(Cp_2M–E) = E^M_{prep} + E^E_{prep} + E^0 + E_{a1} + E_{b1} + E_{b2}$, where $E^0 = E_{el} + E_{Pauli}$.

charge transferred from M $1a_1$ to E *n*p ranges from 1.66 e for O to 1.37 e for Te, while the in-plane back-donation increases in terms of charge from 0.51 e for O to 0.76 e in the case of the more reducing Te. As indicated by the last column in Table 5, the charge separation is greatest for the more polar Ti–O bond and decreases steadily towards the Ti–Te member of the series.

Since the reason for carrying out these computations was to probe the grounds for our failure to capture [Cp^*_2Ti(Te)] when [Cp^*_2Zr(Te)] has been trapped, we have also considered the two zirconium terminal chalcogenides [Cp_2Zr(O)] and [Cp_2Zr(Te)]. The $D(Cp_2M-E)$ bond energies obtained for [Cp_2Zr(O)] and [Cp_2Zr(Te)] are given in Table 3; the data show that the M–E bonds are stronger for the heavier zirconium homologues, especially in the case of tellurium. The reasons for this are complex.[34] Essentially, for titanium the 3d valence orbitals have a similar radial extent to that of the 3s and 3p core orbitals. The 3s and 3p core orbitals will, as a result, contribute to the steric repulsion by four-electron two-orbital interactions with the occupied p_E orbitals at distances where the 3d to p_E bonding overlaps are optimal. For zirconium, the 4s and 4p core are contracted compared with 4d and will not result in comparable repulsive interactions at the optimal distance for the 4d to p_E bonding overlaps; thus, the destabilizing E_{steric} term of Equation (9) is smaller when M = Zr than when M = Ti, and stronger M–E bonds result (Table 3). That the Zr–Te bond is inherently more thermodynamically stable than Ti–Te is part of the explanation for the relative accessibility of [Cp^*_2Zr(Te)] vs. [Cp^*_2Ti(Te)].

Computational experiments on the first excited triplet states of [Cp_2M-E] (M = Ti, Zr; E = O, Te) indicate that [Cp^*_2Ti(Te)] may also be kinetically unstable in the presence of other triplet species. All Cp_2M-E systems studied have singlet ground states with a $(1a_1)^2(1b_2)^2(1b_1)^2$ configuration (Fig. 5). The three occupied orbitals are p_E-based and stabilized by interaction with the metal d components. The lowest unoccupied molecular orbital (LUMO) is $2a_1$, which is an essentially nonbonding d-orbital on the metal; thus, the first excited state is the triplet $^3B_1$ with the $(1a_1)^2(1b_2)^2(1b_1)^1(2a_1)^1$ configuration. Geometrical parameters for each of the species studied are included in Table 4 (in parentheses) for comparison with the singlet ground states. In general, the triplet has a longer M–E distance than the singlet, since an electron is promoted from the weakly M–E bonding $1b_1$ orbital to the nonbonding metal orbital $1a_1$. The M–Cp distance is also affected (it is shorter in the triplets) because the occupation of the M–Cp antibonding $1b_1$ orbital is decreased.

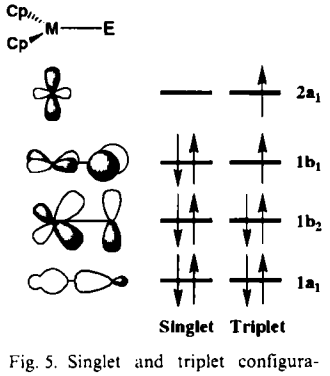

Fig. 5. Singlet and triplet configurations for Cp_2M-E (M = Ti, Zr; E = O, S, Se, Te).

As seen in the last column of Table 4, the calculated energy gap between the $^1A_1$ ground state and the $^3B_1$ triplet is smallest for [Cp_2Ti(Te)]. This is understandable, as the $1b_1$ orbital here is composed of the p_E component with the highest energy. Further, the titanium d orbitals are contracted and less efficient in providing stabilizing interactions than the 4d and 5d orbitals of the heavier congeners.

For [Cp^*_2M(Te)] derivatives, the triplet state may thus be readily accessible thermally or under irradiation with visible light. It represents a highly reactive biradical state of [Cp^*_2M(Te)] (Scheme 3B) that may react rapidly with other triplet species present (for example [Cp^*_2Ti], elemental Te, or even itself), preferentially over two-electron-donor trapping reagents such as the pyridine bases employed in related chemistry. Since the triplet is most accessible to the Ti–Te member of this family of compounds, reactions with other triplet species are most favourable for [Cp^*_2Ti(Te)]. While the singlet–triplet gap for [Cp_2Zr(Te)] is also quite small, the zirconium centre is, by virtue of its larger atomic radius, more sterically accessible to pyridine-base trapping agents than is the titanium centre in [Cp^*_2Ti(Te)].

Conclusions

There are probably three factors that influence whether or not [Cp^*_2M(E)] complexes may be successfully trapped: 1) the bond strength of M–E; 2) the size of the singlet–triplet energy gap; and 3) the steric accessibility of the metal centre for incoming trapping agents. For M = Ti and E = Te, these factors conspire to make [Cp^*_2Ti(Te)] untrappable by pyridine bases; perhaps other less sterically demanding bases (e.g., RNC) will be more successful. In the absence of trapping base, [Cp^*_2Ti(Te)] is, by virtue of a rather weak Ti–Te bond (258.5 kJ mol^{-1}, Table 3), thermodynamically unstable towards loss of Te(0) and formation of **1b** [note the production of elemental tellurium in the reaction of Eq. (6)].[35] The small singlet–triplet gap provides a kinetic path for this reaction (Scheme 4). Dimerization of the

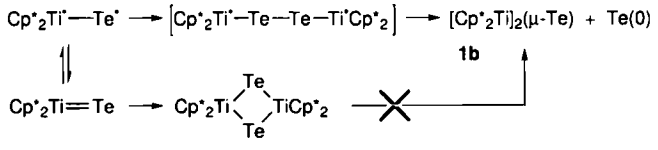

Scheme 4. Pathways for dimerization of [Cp^*_2Ti(Te)].

triplet, favoured sterically because of the bulky Cp* ligands, leads to an intermediate which would be expected to be unstable towards loss of Te; dimerization of the singlet would lead to the $(\mu$-Te$)_2$ dimer,[36] which should be accessible on the basis of the existence of [$(Cp^*_2Ti)_2(\mu$-Se$)_2$].[37]

At the other end of the Ti–E series, the singlet–triplet gap is substantial, the Ti–O bond is very strong, and because oxygen is much smaller than tellurium pyridine can "get in" to trap the terminal oxo derivative effectively.[8] To our knowledge, the remaining members of the titanium series (E = S and Se) have not been trapped successfully; based on our results we would predict that the sulfur species should be trappable. The terminal selenide may be more difficult to apprehend, but our observation of a peak in the mass spectrum of **2a** corresponding to "[Cp^*_2Ti(Se)]" coupled with the isolation of its dimer[38] suggests that [Cp^*_2Ti(Se)(L)] should be synthetically obtainable. The experiments and computations reported herein indicate that, in addition to being inherently thermodynamically unstable, [Cp^*_2Ti(Te)] is also not reactive enough towards even marginally sterically demanding Lewis bases to be trapped prior to reacting with other (triplet) species present in the system.

Experimental Section

General considerations: All reactions were performed under an atmosphere of dinitrogen, which was purified by passage through a glass tower containing MnO on vermiculite and 4 Å molecular sieves separated by a plug of glass wool and a layer

of glass beads. Air-sensitive materials were manipulated and handled in an argon-filled Braun MB150 inert atmosphere glove box or by means of standard Schlenk and vacuum-line techniques [38]. The term "reactor bomb" refers to a cylindrical, thick-walled, round-bottomed Pyrex vessel equipped with a 5 mm Kontes needle valve. Sealable NMR tubes are standard 5 mm NMR tubes that have been equipped with a ground-glass joint.

Materials were purchased from Aldrich and used as received or purified by standard techniques [39]. The reagents $TiCl_3(THF)_3$ [40], [Cp*MgCl(THF)] [41], [Cp^*_2TiCl] [42], [Cp^*_2TiH] [10], [Cp^*_2Ti] [28], [$Cp^*_2Ti(CO)_2$] [43], and $Bu_3P(Te)$ [44] were obtained by literature procedures. Hydrogen gas was obtained from BOC (Canada) and purified by passage though the glass purifying tower described above. Solvents were purified by distillation from either $LiAlH_4$ (hexanes), CaH_2 (CH_2Cl_2) or sodium benzophenone ketyl (benzene, toluene, THF, diethylether) and stored in evacuated pots over "titanocene" or sodium benzophenone ketyl. Deuterated NMR solvents were purchased from Cambridge Isotopes and dried by the same procedures as the protic solvents.

Melting points were determined on a Mel-Temp apparatus in sealed capillaries under argon and are uncorrected. Routine ^1H (200 and 400 MHz) and $^{13}C\{^1H\}$ (100.570) NMR spectra were recorded with C_6D_6 solutions (unless otherwise noted) at ambient temperatures and referenced to C_6D_5H at $\delta = 7.15$ (^1H NMR) and 128.00 ($^{13}C\{^1H\}$ NMR). $^{125}Te\{^1H\}$ (126.4 MHz) and $^{123}Te\{^1H\}$ (104.8 MHz) and $^{77}Se\{^1H\}$ (76.4 MHz) spectra were referenced to external standards Me_2Te ($\delta = 0.0$) and Me_2Se ($\delta = 0.0$), respectively. Solid-state MAS $^{125}Te\{^1H\}$ spectra were also referenced externally to Me_2Te ($\delta = 0$). EPR spectra were recorded on a Varian E-Line Century Series spectrometer and referenced to DPPH (2,2-di(4-*tert*-octylphenyl)-1-picrylhydrazyl, $g = 2.0037$). Mass spectra were obtained on a Kratos MS-890 instrument. Room-temperature magnetic susceptibility measurements were performed on a Johnson Matthey MK II benchtop susceptibility balance by Prof. S. Gambarotta (Ottawa) and variable temperature measurements were carried out by Prof. M. Greenblatt (Rutgers). Elemental analyses were performed by Oneida Research Services (Whitesboro, New York).

Preparation of $[(Cp^*_2Ti)_2(\mu\text{-Se})]$ (1a): [Cp^*_2TiH] (400 mg, 1.3 mmol) and elemental selenium (48 mg, 0.65 mmol) were loaded into a 25 mL round-bottomed flask and attached to a swivel frit apparatus. The assembly was attached to a vacuum line and evacuated, and hexanes (ca. 15 mL) were transferred into the vessel at −78 °C. The solution was allowed to warm to room temperature while being stirred. As the solution approached room temperature, gas evolution was observed, accompanied by a gradual colour change from deep red to dark brown. The reaction mixture was stirred for 3 h and the solvent volume was reduced in vacuo. The dark brown crystalline solid was suspended in hexanes, isolated by filtration and dried in vacuo. Yield: 431 mg, 74% of $[(Cp^*_2Ti)_2(\mu\text{-Se})]$. ^1H NMR: $\delta = 15.4$ (brs, fwhm 2226 Hz, C_5Me_5); $C_{40}H_{60}Ti_2Se$ (715.674): calcd C 67.07, H 8.45; found C 66.90, H 8.87.

Preparation of $[(Cp^*_2Ti)_2(\mu\text{-Te})]$ (1b): [Cp^*_2TiH] (927 mg, 2.9 mmol) and elemental tellurium (185 mg, 0.5 equiv) were loaded into a 25 mL round-bottomed flask and attached to a swivel frit apparatus. The assembly was attached to a vacuum line and evacuated, and toluene (ca. 10 mL) was transferred into the vessel at −196 °C. Upon thawing the solution began to froth vigorously and its colour changed from a deep red to dark brown. The reaction mixture was stirred for 1 h, the toluene was removed in vacuo and hexanes (ca. 5 mL) were condensed in at −78 °C. The dark brown crystalline material was isolated by filtration and dried in vacuo. Yield: 755 mg, 68% of $[(Cp^*_2Ti)_2(\mu\text{-Te})]$. M.p. 311–313 °C (decomp.); ^1H NMR: $\delta = 16.7$ (brs, fwhm 300 Hz, C_5Me_5); ^2H NMR (61.390 MHz): $\delta = 15.9$ (brs, fwhm 13.5 Hz, C_5Me_5); EI-MS: $m/e = 766$ [M^+]; μ_{eff} (298 K) = 2.01 μ_B, μ_{eff} (80–250 K) = 2.1 μ_B; EPR (hexanes, 298 K): $g = 2.0$ (brs); UV/Vis (hexanes): λ_{max}, nm (ε, L mol^{-1} cm^{-1}) = 580 (4000), 470 (12000), 425 (9000), 366 (8000); $C_{40}H_{60}Ti_2Te$ (764.314): calcd C 62.86, H 7.91; found C 62.87, H 7.64.

Preparation of $[Cp^*_2Ti(\eta^2\text{-}Se_2)]$ (2a): [Cp^*_2TiH] (1.58 g, 5 mmol) and elemental selenium (783 mg, 10 mmol) were loaded into a 100 mL round-bottomed flask and attached to a swivel frit apparatus. The assembly was attached to a vacuum line and evacuated, and toluene (ca. 70 mL) was transferred into the vessel at −78 °C. Upon being warmed to room temperature while stirred, the solution began to bubble as its colour changed from a deep red to yellow-black. The reaction mixture was stirred for 2 h, the solution was filtered and the toluene was removed in vacuo. Hexanes (ca. 5 mL) were condensed in at −78 °C and the solid was isolated by filtration and dried in vacuo. Pure samples were obtained by high vacuum sublimation to a water-cooled probe at 60–70 °C. Yield: 1.700 g, 72%. ^1H NMR: $\delta = 1.91$ (s, C_5Me_5); $^{13}C\{^1H\}$ NMR: $\delta = 126.13$, 13.31; $^{77}Se\{^1H\}$ NMR: $\delta = 1252$; EIMS: $m/e = 478$ [M^+]; $C_{20}H_{30}TiSe_2$ (476.277): calcd C 50.44, H 6.35; found C 50.62, H 6.17.

Preparation of $[Cp^*_2Ti(\eta^2\text{-}Te_2)]$ (2b): [Cp^*_2TiH] (507 mg, 1.6 mmol) and $Bu_3P(Te)$ (1.05 g, 3.2 mmol) were loaded into a 25 mL round-bottomed flask and attached to a swivel frit apparatus. The assembly was attached to a vacuum line and evacuated, and toluene (ca. 15 mL) was transferred into the vessel at −196 °C. Upon thawing the solution began to bubble vigorously and its colour changed from a deep red to dark reddish-brown. The reaction mixture was stirred for 30 min and the toluene was removed in vacuo; hexanes (ca. 5 mL) were added by vacuum transfer. The black crystalline material was isolated by filtration and dried in vacuo. Pure samples were obtained by high-vacuum sublimation to a water-cooled probe at 60–70 °C. Yield: 705 mg, 78%. ^1H NMR: $\delta = 2.13$ (s, C_5Me_5); $^{13}C\{^1H\}$ NMR: $\delta = 127.7$, 15.8; $^{125}Te\{^1H\}$ NMR: $\delta = 1463$; $^{123}Te\{^1H\}$ NMR: $\delta = 1462$, $^1J(Te,Te) = 1603$ Hz); $^{125}Te\{^1H\}$ CPMAS NMR (63.2 MHz): $\delta = 1480$; EI-MS: $m/e = 574$ [M^+]; $C_{20}H_{30}TiTe_2$ (573.557): calcd C 41.92, H 5.25; found C 41.88, H 5.27.

Generation of $[Cp^*_2Ti(\eta^2\text{-}TeSe)]$ (2c):

Method A: $[Cp^*_2Ti(\eta^2\text{-}Se_2)]$ (12.0 mg, 0.025 mmol) was loaded into a 5 mm NMR tube and dissolved in C_6D_6 (ca. 0.4 mL). To this solution was added $Bu_3P(Te)$ (8.3 mg, 0.025 mmol) as a C_6D_6 solution (ca. 0.3 mL). The NMR tube was capped and shaken. The colour of the solution immediately changed from yellow-brown to dark red. The ^1H, ^{125}Te and ^{77}Se NMR spectra were immediately obtained and revealed a mixture of $[Cp^*_2Ti(\eta^2\text{-}Te_2)]$ ($\delta = 2.13$), $[Cp^*_2Ti(\eta^2\text{-}Se_2)]$ ($\delta = 1.90$) and $[Cp^*_2Ti(\eta^2\text{-}TeSe)]$ in a ratio of 1:1:3. $[Cp^*_2Ti(\eta^2\text{-}TeSe)]$ ^1H NMR: $\delta = 2.03$ (s, C_5Me_5); $^{77}Se\{^1H\}$ NMR: $\delta = 992$, $^1J(Se,Te) = 683$ Hz); $^{125}Te\{^1H\}$ NMR: $\delta = 2012$. Also present in the NMR were signals for $Bu_3P(Se)$.

Method B: $[Cp^*_2Ti(\eta^2\text{-}Se_2)]$ (11.2 mg, 0.024 mmol) and $[Cp^*_2Ti(\eta^2\text{-}Te_2)]$ (13.5 mg, 0.024 mol) were loaded into a sealable NMR tube. The mixture was dissolved in C_6D_6 (ca. 0.7 mL) and the tube flame-sealed. The sample was heated in a thermostatted bath at 40 °C for 1 h and the ^1H, ^{125}Te and ^{77}Se NMR spectra were immediately recorded, revealing a mixture of **2a**, **2b** and **2c** in a ratio of 1:1:3.

Preparation of $[Cp^*_2Ti(\eta^2\text{-}Se_3)]$ (3): [Cp^*_2TiH] (493 mg, 1.6 mmol) and elemental selenium (366 mg, 4.8 mmol) were loaded into a 50 mL reactor bomb. The reactor bomb was attached to a vacuum line and evacuated, and toluene (ca. 10 mL) was transferred into the vessel at −78 °C. Upon being warmed to room temperature and stirred, the solution began to bubble. The reaction mixture was stirred for 4 d; the solution was then transferred to a swivel frit apparatus and filtered, and the toluene was removed in vacuo. Hexanes (ca. 4 mL) were condensed in at −78 °C and insoluble solid was isolated by filtration and dried in vacuo. Yield: 603 mg (80% pure by ^1H NMR). ^1H NMR: $\delta = 1.75$ (C_5Me_5); $^{13}C\{^1H\}$ NMR: $\delta = 120.99$, 13.31; $^{77}Se\{^1H\}$ NMR: $\delta = 813$ (2Se, $^1J(Se,Se) = 162.4$ Hz), 322 (1Se); EI-MS: $m/e = 556$ [M^+].

Conversion of $[Cp^*_2Ti(\eta^2\text{-}Se_3)$ to $[Cp^*_2Ti(\eta^2\text{-}Se_2)$ with Ph_3P: $[Cp^*_2Ti(\eta^2\text{-}Se_3)]$ (15 mg, 0.027 mmol) and Ph_3P (7.1 mg, 0.027) were loaded into a 5 mm NMR tube and dissolved in C_6D_6 (ca. 0.7 mL). The NMR tube was capped and shaken. Upon mixing the colour of the solution changed from yellow-brown to dark red instantaneously. The ^1H NMR spectrum was recorded and showed complete conversion to **2a**.

Conversion of $[Cp^*_2Ti(\eta^2\text{-}Se_2)]$ to $[(Cp^*_2Ti]_2(\mu\text{-Se})]$ with Me_3P: $[Cp^*_2Ti(\eta^2\text{-}Se_2)]$ (14.8 mg, 0.031 mmol) was loaded into a sealable 5 mm NMR tube. The NMR tube was fitted with a 180° needle valve adapter and attached to a vacuum line; PMe_3 (1 equiv) was condensed into the tube at −196 °C by means of a calibrated volume bulb. The tube was flame-sealed and allowed to warm to room temperature. Upon being warmed, the colour of the solution changed from dark red to red-brown. The ^1H NMR spectrum indicated quantitative conversion to **1a**.

Conversion of $[Cp^*_2Ti(\eta^2\text{-}Te_2)]$ to $[(Cp^*_2Ti)_2(\mu\text{-Te})]$ with Hg(0): $[Cp^*_2Ti(\eta^2\text{-}Te_2)]$ (500 mg, 0.87 mmol) and elemental mercury (ca. 1 mL) were loaded into a 50 mL reactor bomb. The reactor bomb was attached to a vacuum line and evacuated, and toluene (ca. 20 mL) was transferred into the vessel at −78 °C. The reaction mixture was stirred for 3 d. The solution was transferred to a swivel frit apparatus and filtered; **1b** was isolated as described above. Yield 285 mg, 86% of **1b**.

Conversion of $[Cp^*_2Ti(\eta^2\text{-}Te_2)$ to $[(Cp^*_2Ti)_2(\mu\text{-Te})]$ with $[Cp^*_2TiH]$: $[Cp^*_2Ti(\eta^2\text{-}Te_2)]$ (11.6 mg, 0.020 mmol) and $[Cp^*_2TiH]$ (19.4 mg, 0.06 mmol) were loaded into a 5 mm NMR tube and dissolved in C_6D_6 (ca. 0.8 mL). The NMR tube was capped and shaken, and vigorous bubbling occurred along with an instantaneous colour change from dark red to dark brown. The ^1H NMR spectrum showed complete conversion to **1b**.

Conversion of $[(Cp^*_2Ti)_2(\mu\text{-Te})]$ to $[Cp^*_2Ti(\eta^2\text{-}Te_2)]$ with $Bu_3P(Te)$: $[(Cp^*_2Ti)_2(\mu\text{-Te})]$ (134 mg, 0.18 mmol) and $Bu_3P(Te)$ (174 mg, 0.56 mmol) were loaded into a 25 mL round-bottomed flask and attached to a swivel frit apparatus. The assembly was attached to a vacuum line and evacuated, and toluene (ca. 10 mL) was transferred into the vessel at −78 °C. The mixture was stirred for 3 h, and **2b** was isolated as described above. Yield 153 mg, 77% of **2b**.

Reaction of $[Cp^*_2Ti(\eta^2\text{-}Te_2)]$ with Hg(0) in the presence of pyridine: $[Cp^*_2Ti(\eta^2\text{-}Te_2)]$ (0.300 g) and elemental mercury (ca. 1 mL) were loaded into a 50 mL round-bottomed flask and attached to a swivel frit apparatus. The assembly was attached to a vacuum line and evacuated, and toluene (ca. 20 mL) was transferred into the vessel at −78 °C. Dry pyridine was added neat in 100-fold excess. The mixture was stirred for 3 d, over which time a gray precipitate was deposited. The reaction mixture was filtered and the volatiles were removed in vacuo. ^1H NMR analysis of the remaining solids revealed the presence of only **1b**; no diamagnetic Cp*-containing products were observed.

Reaction of $[Cp^*_2Ti$ with $[Cp^*_2Ti(\eta^2\text{-}Te_2)]$: $[Cp^*_2Ti]$ (4.0 mg, 0.013 mmol) and $[Cp^*_2Ti(\eta^2\text{-}Te_2)]$ (7.2 mg, 0.013 mmol) were loaded into a 5 mm NMR tube and dissolved in C_6D_6 (ca. 0.8 mL). Upon mixing an immediate reaction occurred that turned the solution from dark red to dark brown. The ^1H NMR spectrum indicated partial conversion of the **2b** to **1b**. Addition of a further 0.026 mmol of $[Cp^*_2Ti]$ (8.0 mg) resulted in complete conversion to **1b**.

Reaction of $[Cp^*_2Ti$ with elemental tellurium: $[Cp^*_2Ti]$ (7.0 mg, 0.022 mmol) and elemental tellurium (4.0 mg, excess) were loaded into a 5 mm NMR tube and dissolved in C_6D_6 (ca. 0.8 mL). The NMR tube was capped and shaken. An immediate reaction occurred which turned the solution from orange to dark brown. The ^1H NMR spectrum showed complete conversion of the $[Cp^*_2Ti]$ to **1b**.

Reactions of $[Cp^*_2Ti$ with $Bu_3P(Te)$: $[Cp^*_2Ti]$ (4.2 mg, 0.013 mmol) and $Bu_3P(Te)$ (2.2, 4.4 or 8.8 mg, 0.5–2 equiv) were loaded into 5 mm NMR tubes and dissolved in C_6D_6 (ca. 0.8 mL). An immediate reaction occurred in each case that turned the solution from orange to dark brown to red. The ^1H NMR spectra indicated conversion of the $[Cp^*_2Ti]$ to mixtures of **1b** and **2b** in the molar ratios of 1:0, 2:1 and 0:1, for 0.5, 1.0 and 2.0 equiv of Te, respectively.

Reaction of $[Cp^*_2Ti(CO)_2]$ with elemental tellurium in the presence of pyridine: $[Cp^*_2Ti(CO)_2]$ (183 mg, 0.49 mmol) and elemental tellurium (62 mg, 0.49 mmol) were loaded into a 50 mL reactor bomb. The vessel was evacuated and approx. 20 mL toluene was added by vacuum transfer. Under a flow of nitrogen, dry pyridine (1 mL, excess) was syringed into the vessel. The mixture was stirred for 3 d at room temperature, over which time the colour of the solution changed from orange to dark red. The volatiles were removed in vacuo and a ^1H NMR spectrum of the residues was recorded, which indicated only the presence of $[Cp^*_2Ti(CO)_2]$ and **2b**.

Computational details: All calculations were based on the Amsterdam density functional package ADF [33,34,45] developed by Baerends et al. and vectorized by Ravenek. The adopted numerical integration scheme was that developed by te Velde et al. [46d,e].

The titanium and zirconium metal centres were described by an uncontracted triple-ζ STO basis set [46,47] for the outer *ns*, *np*, *nd*, $(n+1)$s and $(n+1)$p orbitals, whereas the shells of lower energy were treated by the frozen core approximation [33]. The *ns* and *np* valence orbitals on the chalcogens were described by an uncontracted double-ζ STO basis augmented by a single 3d; lower-energy shells were treated by the frozen core approximation. A double-ζ basis set augmented by one 2p polarization function was employed for hydrogen. A number of auxiliary s, p, d, f and g STO functions centred on all nuclei were used in order to fit the molecular density and present Coulomb and exchange potentials accurately in each SCF cycle [48].

The self-consistent DFT calculations were carried out by augmenting the local exchange-correlation potential of Vosko et al. [49] with Becke's [50] nonlocal exchange corrections and Perdew's [51] nonlocal correlation correction (NL-SCF). All structures were optimized within C_{2v} symmetry based on the algorithms developed by Versluis and Ziegler [52].

X-ray structural analysis of 1b and 2b: Single crystals were mounted in thin-walled glass capillaries and optically centred in the X-ray beam of an Enraf–Nonius CAD-4 diffractometer. Unit cell dimensions were determined by least-squares refinement of the setting angles of 24 high angle reflections and intensity data were collected by the $\omega-2\theta$ scan mode. Data were corrected for Lorentz, polarization and absorption effects but not for extinction [53].

1b: $C_{40}H_{60}Ti_2Te$, $0.20\times0.25\times0.30$ mm, triclinic, $P\bar{1}$, $a = 8.9445(17)$ Å, $b = 12.186(2)$ Å, $c = 18.876(4)$ Å, $\alpha = 77.35(4)^\circ$, $\beta = 83.60(3)^\circ$, $\gamma = 73.638(20)^\circ$, $V = 1923.4(6)$ Å^3, $Z = 2$, $\rho_{calc} = 1.32$ mg m^{-3}, $2\theta_{max} = 45^\circ$, $Mo_{K\alpha}$ radiation, $\lambda = 0.70930$ Å, omega scan mode, $T = 298$ K, 5194 measured reflections, 5013 independent, 2671 reflections with $I_{net} > 3.0\sigma(I_{net})$, $\mu = 1.18$ mm^{-1}, min/max transmission = 0.793 and 0.990, $R(F) = 0.056$, $R_w = 0.055$, GoF = 2.24. After anisotropic refinement of all non-hydrogen atoms, methyl hydrogen atoms were located by inspection of a difference Fourier map and fixed (temperature factors being based upon the carbon to which they were bonded).

2b: $C_{20}H_{30}TiTe_2$, $0.30\times0.30\times0.35$ mm, orthorhombic, *Fdd*2, $a = 9.266(4)$ Å, $b = 16.902(7)$ Å, $c = 27.356(14)$ Å, $V = 4265(3)$ Å^3, $Z = 8$, $\rho_{calc} = 1.79$ mg m^{-3}, $2\theta_{max} = 50^\circ$, $Mo_{K\alpha}$ radiation, $\lambda = 0.70930$ Å, ω scan mode, $T = 298$ K, 1054 measured reflections, 1039 independent, 949 reflections with $I_{net} > 3.0\sigma(I_{net})$, $\mu = 1.18$ mm^{-1}, min/max transmission = 0.765 and 0.998, $R(F) = 0.037$, $R_w = 0.044$, GoF = 2.92. After anisotropic refinement of all non-hydrogen atoms, methyl hydrogen atoms were located by inspection of a difference Fourier map and fixed, temperature factors being based upon the carbon atoms to which they are bonded. The enantiomorph was fixed by including Friedel reflections in the least-squares refinement and refining Rogers chirality η [54]. A value of 1.1 was obtained for chirality η. A weighting scheme based upon counting statistics was used with the weight modifier k in kF_o^2 being determined by evaluation of variation in the standard reflections obtained during the course of data collection. Neutral atom scattering factors were taken from ref. [55]. Values of R and R_w are given by $R = (F_o - F_c)/\sum F_o$ and $R_w = [\sum(w(F_o - F_c))^2/\sum(wF_o^2)]^{1/2}$. All crystallographic calculations were conducted with the PC version of the NRCVAX program package locally implemented on an IBM-compatible 80486 computer [56].

Acknowledgments: Funding for this work was provided by the Natural Sciences and Engineering Research Council of Canada in the form of research grants to WEP, TZ and MJZ. WEP thanks Prof. T. Cundari (Memphis) for disclosure of results prior to publication and helpful discussions.

Received: April 12, 1996 [F350]

[1] a) L. C. Roof, J. W. Kolis, *Chem. Rev.* **1993**, *93*, 1037; b) M. Draganjac, T. B. Rauchfuss, *Angew. Chem.* **1985**, *97*, 745; *Angew. Chem. Int. Ed. Engl.* **1985**, *24*, 742; c) C. M. Bolinger, T. B. Rauchfuss, *Inorg. Chem.* **1982**, *21*, 3947.
[2] A. Shaver, J. M. McCall, G. Marmolejo, *Inorg. Synth.* **1990**, *27*, 59.
[3] E. W. Abel, M. Booth, K. G. Orrell, *J. Organomet. Chem.* **1978**, *160*, 75.
[4] a) D. M. Giolando, M. Papavassiliou, J. Pickardt, T. B. Rauchfuss, R. Steudel, *Inorg. Chem.* **1988**, *27*, 2596; b) D. M. Giolando, T. B. Rauchfuss, A. L. Rheingold, S. R. Wilson, *Organometallics* **1987**, *6* , 667.
[5] a) W. A. Howard, G. Parkin, *J. Am. Chem. Soc.* **1994**, *116*, 606; b) W. A. Howard, G. Parkin, *J. Organomet. Chem.* **1994**, *472*, C1; c) M. J. Carney, P. J. Walsh, R. G. Bergman, *J. Am. Chem. Soc.* **1990**, *112*, 6426; d) M. J. Carney, P. J. Walsh, F. J. Hollander, R. G. Bergman, *Organometallics* **1992**, *11*, 761.
[6] W. A. Howard, G. Parkin, A. L. Rheingold, *Polyhedron* **1995**, *14*, 25.
[7] M. T. Benson, T. R. Cundari, S. J. Lim, H. D. Nguyen, K. Pierce-Beaver, *J. Am. Chem. Soc.* **1994**, *116*, 3955.
[8] M. R. Smith, P. T. Matsunaga, R. A. Andersen, *J. Am. Chem. Soc.* **1993**, *115*, 7049.
[9] J. M. Fischer, W. E. Piers, L. R. MacGillivray, M. J. Zaworotko, *Inorg. Chem.* **1995**, *34*, 2499.
[10] G. A. Luinstra, J. H. Teuben, *J. Am. Chem. Soc.* **1992**, *114*, 3361.
[11] J. M. Fischer, W. E. Piers, S. D. Pearce-Batchilder, M. J. Zaworotko, *J. Am. Chem. Soc.* **1996**, *118*, 283.
[12] W. W. Lukens, R. A. Andersen, *Inorg. Chem.* **1995**, *34*, 3440.
[13] B. Honold, U. Thewalt, M. Herberhold, H. G. Alt, L. B. Kool, M. D. Rausch, *J. Organomet. Chem.* **1986**, *314*, 105.
[14] R. S. Drago, *Physical Methods for Chemists*, 2nd ed., Saunders, Toronto, **1992**, p. 475.
[15] Owing to the poor solubility of **1** in hydrocarbon solvents, measurement of the magnetic moment in solution by the Evans method was not possible.
[16] a) D. J. Berg, R. A. Andersen, A. Zalkin, *Organometallics* **1988**, *7*, 1858; b) W. E. Piers, D. J. Parks, L. R. MacGillivray, M. J. Zaworotko, *Organometallics* **1994**, *13*, 4547.
[17] J. W. Lauher, R. Hoffmann, *J. Am. Chem. Soc.* **1976**, *98*, 1729.
[18] V. Christou, S. P. Wuller, J. Arnold, *J. Am. Chem. Soc.* **1993**, *115*, 10545.
[19] This value was computed by ECP methods: T. R. Cundari, personal communication.
[20] E = Te: D. Fenske, A. Grissinger, *Z. Naturforsch.* **1990**, *45b*, 1309. E = Se: see ref. [4a].
[21] L. R. Maxwell, V. M. Mosley, *Phys. Rev.* **1940**, *57*, 21.
[22] P. Cherin, P. Unger, *Acta Crystallogr.* **1967**, *23*, 670.
[23] Other monomeric η^2-Se_2 complexes: a) A. P. Ginsberg, W. E. Lindsell, C. R. Sprinkle, K. W. West, R. L. Cohen, *Inorg. Chem.* **1982**, *21*, 3666; b) C. M. Bolinger, T. B. Rauchfuss, *Organometallics* **1982**, *1*, 223; c) D. H. Farrar, K. R. Gruny, N. C. Payne, W. R. Roper, A. Walker, *J. Am. Chem. Soc.* **1979**, *101*, 6577; d) M. Herberhold, D. Reimer, V. Thèwalt, *Angew. Chem. Int. Ed. Engl.* **1983**, *22*, 1000; d) C. Ratti, P. R. A. Tabard, R. Guillard, *J. Chem. Soc. Chem. Commun.* **1989**, 69; f) see ref. [6].
[24] Other monomeric η^2-Te_2 complexes: a) J. H. Shin, G. Parkin, *Organometallics* **1994**, *13*, 2147; b) D. Rabinovich, G. Parkin, *J. Am. Chem. Soc.* **1993**, *115*, 9822; c) M. Di Vaira, M. Peruzzini, P. Stoppioni, *Angew. Chem. Int. Ed. Engl.* **1987**, *26*, 916; d) see ref. [6].
[25] a) D. Rabinovich, G. Parkin, *Inorg. Chem.* **1995**, *34*, 6341; b) H. C. E. McFarlane, W. McFarlane, *J. Chem. Soc. Dalton Trans.* **1973**, 2416.
[26] P. H. Bird, J. M. McCall, A. Shaver, U. Siriwardan, *Angew. Chem.* **1982**, *94*, 375; *Angew. Chem. Int. Ed. Engl.* **1982**, *21*, 384.
[27] The effect of phosphine basicity on the selectivity of desulfurization reactions of titanocene polysulfides has been noted (see ref. [4b]).
[28] J. E. Bercaw, *J. Am. Chem. Soc.* **1974**, *96*, 5087.
[29] While our efforts focussed on the terminal telluride, we also attempted to prepare the terminal selenide; the experiments for Equations (5) and (6) with E = Se failed to result in generation of $[Cp^*_2Ti{=}Se(py)]$.
[30] Although tellurium has a ^3P ground state, Steigerwald has noted that when transferred from $Te{=}PBu_3$ the tellurium is functionally in an excited-state configuration that is a combination of the ^1D and ^1S states of the atom: M. L. Steigerwald, C. E. Rice, *J. Am. Chem. Soc.* **1988**, *110*, 4288.
[31] a) T. Ziegler, A. Rauk, *Theor. Chim. Acta* **1977**, *46*, 1; b) E. J. Baerends, A. Rozendaal, *NATO ASI* **1986**, *C176*, 159; c) T. Ziegler, *ibid.* **1992**, *C378*, 367.
[32] E. J. Baerends, P. Ros, *Int. J. Quantum Chem. Symp.* **1978**, *12*, 169.
[33] E. J. Baerends, D. E. Ellis, P. Ros, *Chem. Phys.* **1973**, *2*, 41.

0947-6539/96/0210-1228 $ 15.00+.25/0

[34] H. Jacobsen, T. Ziegler, *Comments Inorg. Chem.* **1995**, *17*, 301.
[35] Given the value calculated for D(Ti–Te) in [Cp^*_2Ti(Te)] (260 kJ mol^{-1}), and an estimated D(Te–Te) of 126 kJ mol^{-1} (J. E. Hugheey, R. S. Evans, *J. Inorg. Nucl. Chem.* **1970**, *32*, 383), the Ti–Te bonds of **1b** would have to be approx. 200 kJ mol^{-1} in order for this reaction to be enthalpically favoured.
[36] It has been shown that the compound [{$(C_5H_4tBu)_2Zr$}$_2(\mu$-Te)$_2$] is formed by dimerization of [$(C_5H_4tBu)_2$Zr(Te)]: D. E. Gindelberger, J. Arnold, *Organometallics* **1994**, *13*, 4462.
[37] [$(Cp^*_2Ti)_2(\mu$-Se)$_2$] has been isolated: F. Bottomley, T.-T. Chin, G. O. Egharevba, L. M. Kane, D. A. Pataki, P. S. White, *Organometallics* **1988**, *7*, 1214. No mention of the decomposition of this compound to a paramagnetic species (i.e. **1a**) appeared in this report.
[38] B. J. Burger, J. E. Bercaw, in *Experimental Organometallic Chemistry* (Eds.: A. L. Wayda, M. Y. Darensbourg), *ACS Symp. Ser. 357*; American Chemical Society, Washington, DC, **1987**.
[39] D. D. Perrin, W. L. F. Armarego, *Purification of Laboratory Chemicals*, 3rd ed, Pergamon, New York, **1988**.
[40] P. Sharp, L. E. Manzer, J. Deaton, R. R. Shrock, *Inorg. Synth.* **1982**, *21*, 137.
[41] J. M. Manriquez, P. J. Fagan, E. A. Maatta, A. M. Seyam, T. J. Marks, *J. Am. Chem. Soc.* **1981**, *103*, 6651.
[42] a) J. W. Pattiasina, H. J. Heeres, F. van Bolhuis, A. Meetsma, J. H. Teuben, *Organometallics* **1987**, *6*, 1004; b) G. A. Luinstra, L. C. ten Cate, J. W. Pattiasina, H. J. Heeres, A. Meetsma, J. H. Teuben, *Organometallics* **1991**, *10*, 3227.
[43] J. E. Bercaw, M. Marvich, L. G. Bell, H. H. Brintzinger, *J. Am. Chem. Soc.* **1972**, *94*, 1219.
[44] R. A. Zingaro, B. H. Steeves, K. Irgolic, *J. Organomet. Chem.* **1965**, *4*, 320.
[45] a) E. J. Baerends, P. Ros, *Chem. Phys.* **1973**, *2*, 52; b) G. te Velde, *Amsterdam Density Functional (ADF). User Guide, Release 1.1.3*; Department of Theoretical Chemistry, Free University, Amsterdam, **1994**; c) W. Ravenek, in *Algorithms and Applications on Vector and Parallel Computers* (Eds.: H. J. J. te Riele, T. J. Dekker, H. A. van de Horst), Elsevier, Amsterdam, **1987**; d) P. M. Boerrigter, G. te Velde, E. J. Baerends, *Int. J. Quantum Chem.* **1988**, *33*, 87; e) G. te Velde, E. J. Baerends, *J. Comput. Chem.* **1992**, *99*, 84.
[46] J. G. Snijders, E. J. Baerends, P. Vernoijs, *At. Nucl. Data Tables* **1982**, *26*, 483.
[47] P. Vernoijs, J. G. Snijders, E. J. Baerends, *Slater Type Basis Functions for the Whole Periodic System*, Internal report, Department of Theoretical Chemistry, Free University, Amsterdam, **1981**.
[48] J. Krijn, E. J. Baerends, *Fit Functions in the HFS Method*, Internal report, Department of Theoretical Chemistry, Free University, Amsterdam, **1984**.
[49] S. H. Vosko, L. Wilk, M. Nusair, *Can. J. Phys.* **1980**, *58*, 1200.
[50] A. Becke, *Phys. Rev. A* **1988**, *38*, 3098.
[51] J. Perdew, *Phys. Rev. B* **1986**, *33*, 8822.
[52] L. Versluis, T. Ziegler, *J. Chem. Phys.* **1988**, *88*, 322.
[53] Crystallographic data (excluding structure factors) for the structure reported in this paper have been deposited with the Cambridge Crystallographic Data Centre as supplementary publication no. CCDC-1220-23. Copies of the data can be obtained free of charge on application to the Director, CCDC, 12 Union Road, Cambridge CB21EZ, UK (Fax: Int. code + (1223)336-033; e-mail: teched@chemcrys.cam.ac.uk).
[54] D. Rogers, *Acta Crystallogr.* **1981**, *A37*, 734.
[55] *International Tables for X-ray Crystallography Vol. IV*, Kynoch, Birmingham, **1974**.
[56] E. J. Gabe, Y. Le Page, J.-P. Charland, F. L. Lee, P. S. White, *J. Appl. Crystallogr.* **1989**, *22*, 384.